

Role of Elongation and Secondary Pathways in S6 Amyloid Fibril Growth

SUPPORTING MATERIAL

April 16, 2012

1 AF4

1.1 AF4 detection limit

The asymmetrical flow field-flow fractionation (AF4) system is used to separate S6 species according to size. To test this systems ability to detect potential oligomeric S6 structures, we analysed the sensitivity of our AF4 absorbance and multi-angle light scattering (MALS) detectors.

1.1.1 Analysis of absorbance intensity using standard protein

We prepared a dilution series of 1mg/ml Ribonuclease A (RibA) (13.7kDa, theoretical $\epsilon_{280\text{nm}}^{\text{RibA}} = 8640\text{cm}^{-1}\text{M}^{-1}$). RibA is similar in size to S6 (11 kDa), but its extinction coefficient is slightly lower ($\epsilon_{280\text{nm}}^{\text{S6}} = 12700\text{cm}^{-1}\text{M}^{-1}$). 100 μl of RibA sample was injected onto a 5ml Hitrap desalting column, using 5mM Tris-Cl, 150mM NaCl pH 7.4 at 1ml/min as eluent. We probed the sensitivity of the AF4 instrument using absorbance at 205nm, where proteins show relatively little variability in their extinction coefficients due to amino acid composition[1]. For comparison, the detection limit using absorbance at 280nm was also evaluated. A total RibA protein load of $\sim 410\text{ng}$ gave rise to a peak slightly above the baseline. Injection of 1.2 μg RibA showed a clear increase in absorbance at 205nm and increasing amounts continued to show larger peaks (Fig. S1 A). Thus, it is safe to assume that the detection limit of 205nm absorbance is between 0.41 μg and 1.2 μg which is $\leq 1\%$ of the injected S6 protein (120 μg) in AF4 analysis. We also evaluated the sensitivity

using absorbance at 280nm. Injection of $\sim 410\text{ng}$ RibA did not give rise to a noticeable peak. However, clear peaks were observed on injection of $1.2\mu\text{g}$ RibA and higher concentration indicating that the detection lies around this level (Fig. S1 B). Note that the S6 $\epsilon_{280\text{nm}}$ is approximately 50% larger than the RibA $\epsilon_{280\text{nm}}$, suggesting that the sensitivity to S6 species will be higher than for RibA species.

1.1.2 Analysis of light scattering intensity using polystyrene beads

The light scattering (LS) intensity at a 90 degree scattering angle was used to evaluate the sensitivity of the MALS detector using 19nm polystyrene (PS) standards (Postnova Analytics, Z-PS-POS-001-0.02) separated on the desalting column using 1ml/min 2% SDS solution to avoid particle aggregation. While the lowest concentration assayed (45.2ng) showed 90° LS intensities comparable to the blank injection (2% SDS), the injection of $\sim 136\text{ng}$ of PS particles showed an increase in intensity and the LS intensity continued to increase at increasing particle concentrations (Fig. S2). We emphasize here that the maximum intensity recorded after injection of a $1.2\mu\text{g}$ PS particle suspension is approaching approximately 50% of detector saturation. Thus, oligomeric S6 species of similar size and amount (corresponding to 1% of the total protein) would easily be captured by the MALS detector even though they are close to the threshold value for absorbance detection.

1.2 AF4 measurements

Having demonstrated the sensitivity of our AF4 measurements, we performed AF4 measurements in order to confirm directly whether oligomeric species were present over the time-course of our pre-seeded experiments. We detected no soluble S6 oligomeric species by absorbance or light scattering within 5 days of incubation, as shown in Fig. S3.

We also confirmed that during this time period all of the monomeric S6 protein had aggregated into insoluble fibrils as shown by a decrease in absorbance at 280nm of the S6 monomer peak, a large rise in ThT fluorescence intensity and the presence of a maximum at 1630cm^{-1} in the FTIR spectrum.

2 TEM

We performed TEM measurements to investigate the (2nd generation) fibrillar material grown from pre-formed seeds in our experiments. Firstly, no fibril branching was observed for any of the mutants; for example, images of

3 mutants are displayed in Fig. S4. This implies that the secondary pathway identified in the main text is either filament fragmentation, or a surface catalysed nucleation reaction that does not result in branching. These observations corresponds well with earlier observations for S6 fibrils where branching was not observed[2].

In addition, no oligomeric structures were observed in the second generation samples, with only fibrillar material seen over many images (around 20 pictures).

Interestingly, we observed some bundling of 2nd generation fibrils, Fig. S4, after time scales much longer than that for monomer depletion in the kinetic experiments in the main text. Bundling was not observed for the initial seed solutions, likely due to the disruptive force of sonication with subsequent storage at 4°C.

3 AFM

Images of S6 fibril seeds and mature fibrils grown from seeds were obtained by AFM, Fig. S5, of fibrils grown from seeds. We observed only fibrillar species, and did not detect small oligomers. In addition, we were unable to identify any differences in structure between AFM images of the initial seeds and the final fibrils grown from them, apart from the bundling seen after long time scales for the 2nd generation fibrils already observed in the TEM images.

4 FTIR

Seeds and the fibrils formed from elongation of the seeds (2nd generation fibrils) are expected to give the same fibril structure since they are grown under the same conditions. AFM analysis of seed structures indicate that seeds are a uniform population so polymorphism is not expected. Nevertheless we confirmed directly using FTIR spectras that seeds have similar structure to their corresponding 2nd generation fibrils, Fig. S6.

In addition, we note that S6 monomer and fibril are readily distinguishable by FTIR, Fig. S7. S6 display a small but significant spectral shift in the amide I region. S6 monomers have a spectral maximum at 1638 cm^{-1} whereas S6 fibrils have a spectral maximum at 1630 cm^{-1} corresponding well with other observations for fibril systems[3]. In addition to the spectral shift, the spectra also reveal an additional shoulder at $1700\text{-}1750\text{ cm}^{-1}$ and the Lorentzian fitting clearly show that they are different. All S6 mutants

showed a similar fingerprint as LA30/VA65.

References

- [1] R. K. Scopes, *Measurement of protein by spectrophotometry at 205 nm.*, Anal Biochem **59**, 277 (1974).
- [2] J. S. Pedersen, G. Christensen, D. E. Otzen, *Modulation of S6 fibrillation by unfolding rates and gatekeeper residues.*, J Mol Biol **341**, 575 (2004).
- [3] G. Zandomenighi, M. R. H. Krebs, M. G. McCammon, M. Fndrich, *FTIR reveals structural differences between native beta-sheet proteins and amyloid fibrils.*, Protein Sci **13**, 3314 (2004).

Figure captions

Fig S1. Calibration of the sensitivity of the AF4 absorbance unit using 0.41-33.3 μ g Ribonuclease A. A: absorbance at 205nm. B: absorbance at 280nm.

Fig S2. Light scattering intensity of 0-1.22 μ g polystyrene standards recorded by MALS detector.

Fig S3. Absorbance at 205nm from AF4 measurements, showing that no oligomers are detected within 5 days of incubation. Absorbance at 280nm and light scattering measurements gave identical results.

Fig S4. TEM of S6 fibrils grown from monomer and pre-formed seed of (A) LA30/VA65, (B) IA8, and (C) LA30. Dimensions are 1000 nm x 780 nm.

Fig S5. Representative AFM image of S6 fibrils grown from LA75/MA67 monomeric peptide with LA30/VA65 pre-formed seeds. Small oligomeric species were not observed.

Fig S6. Comparison of normalized FTIR spectra of LA30/VA65 seed (crosses) and 2nd generation fibrils (open circles), showing no significant differences.

Fig S7. Spectra of LA30/VA65 monomers (A) and fibrils (B). Experimental data are displayed as open circles (50% of datapoints shown), components of a Lorentzian fit are displayed as small filled circles and the sum of the components is a continuous line, overlapping the experimental data.

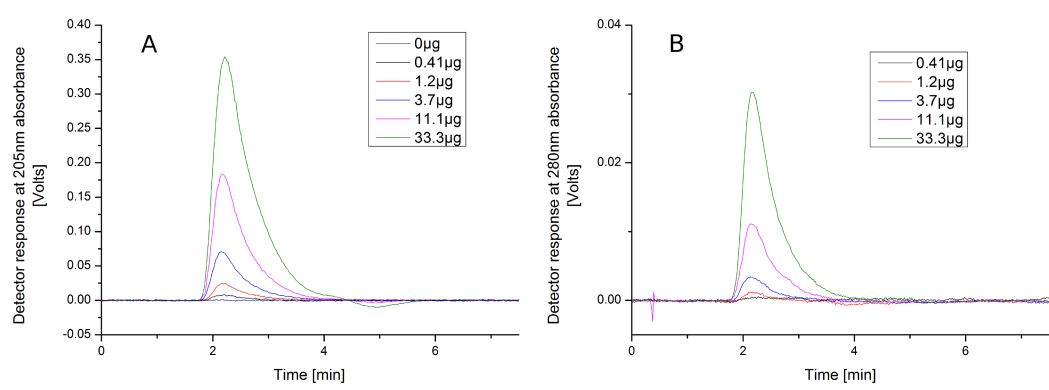


Figure S1:

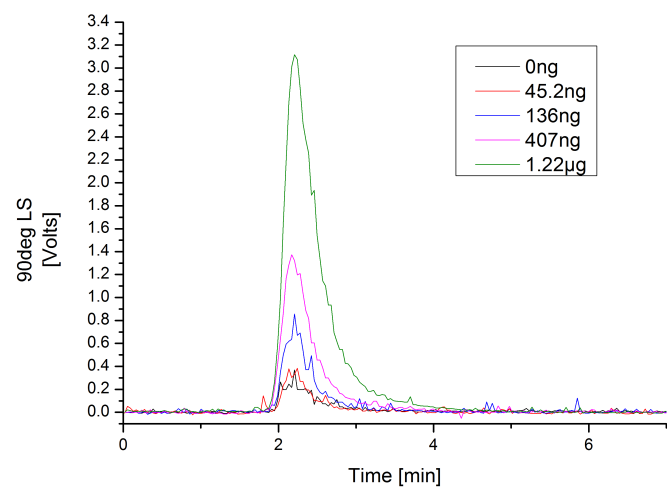


Figure S2:

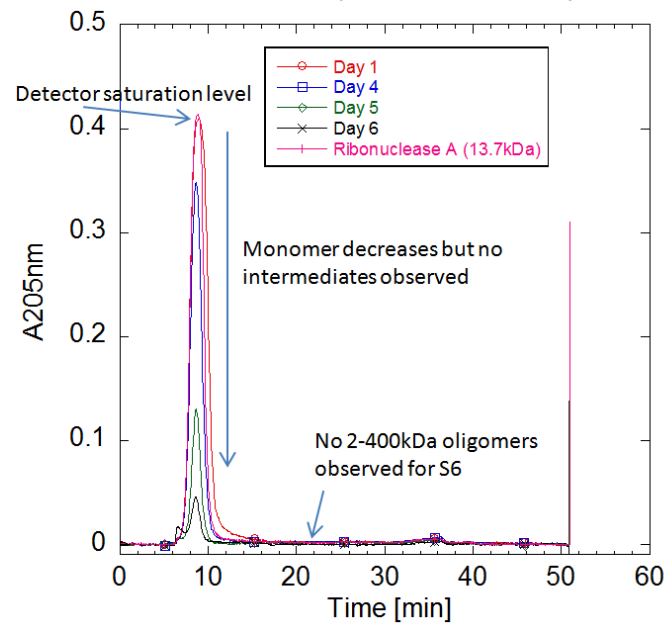


Figure S3:

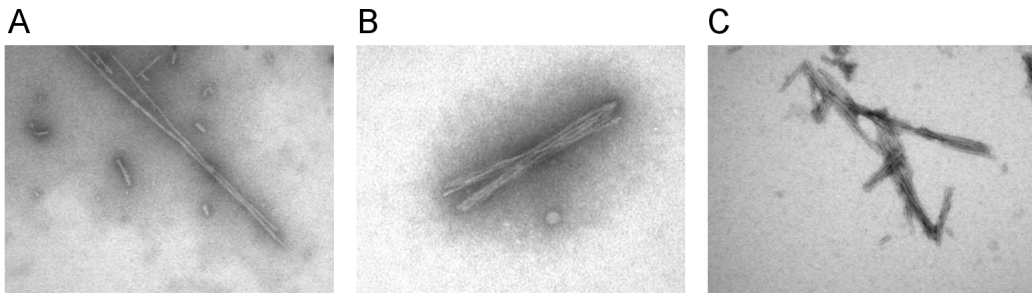


Figure S4:

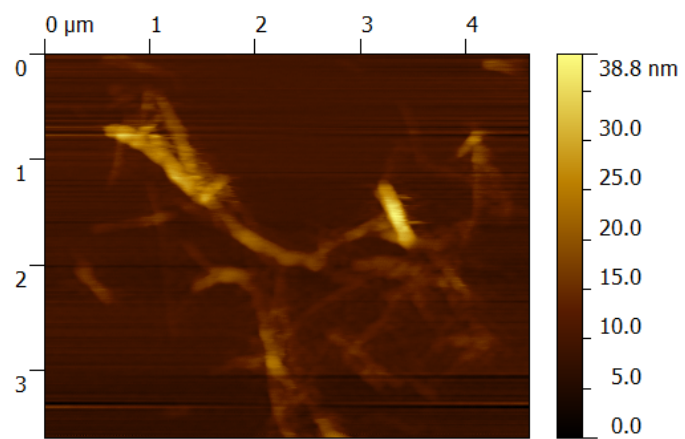


Figure S5:

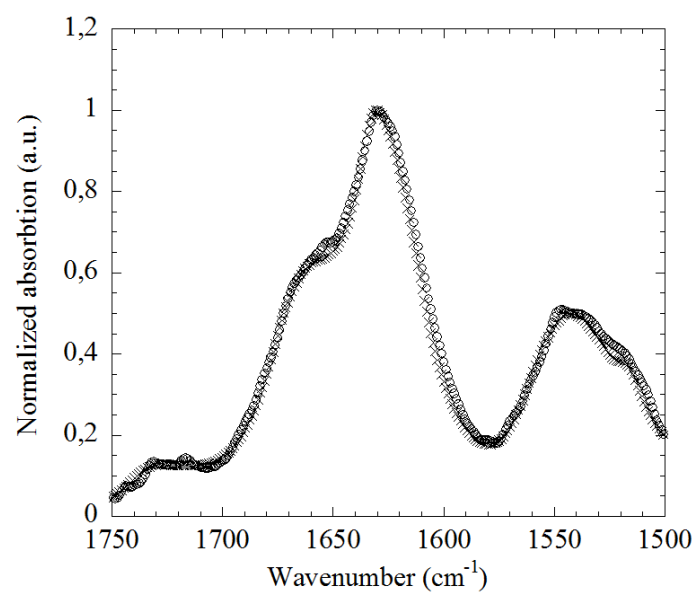


Figure S6:

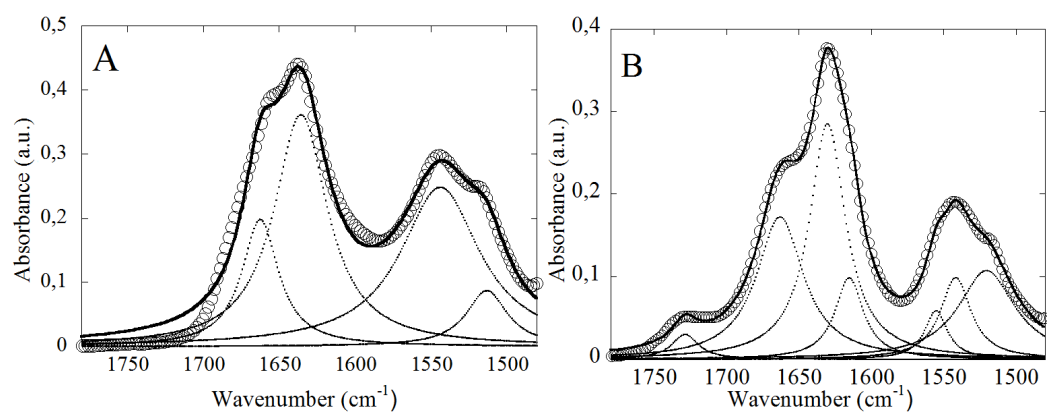


Figure S7: